Pulsar outer-gap model: phase-resolved spectrum of the Crab pulsar

HIROTANI, Kouichi

ASIAA/TIARA, Taiwan

CTA Workshop
ICRR
October 3, 2014

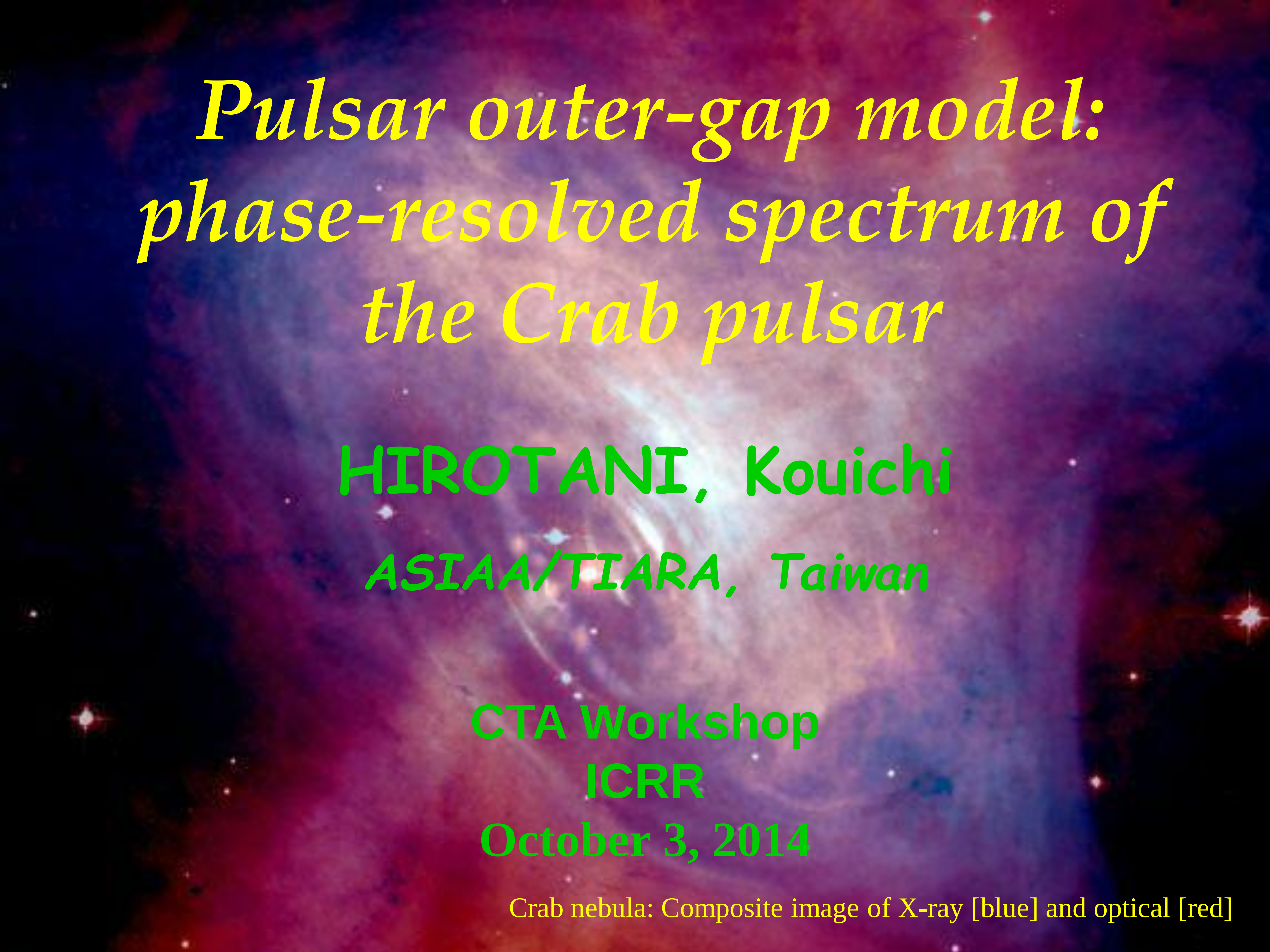

Crab nebula: Composite image of X-ray [blue] and optical [red]

§1 γ-ray Pulsar Observations

After 2008, LAT aboard Fermi has detected more than 117 pulsars above 100 MeV.

Fermi/LAT point sources (>100 MeV)

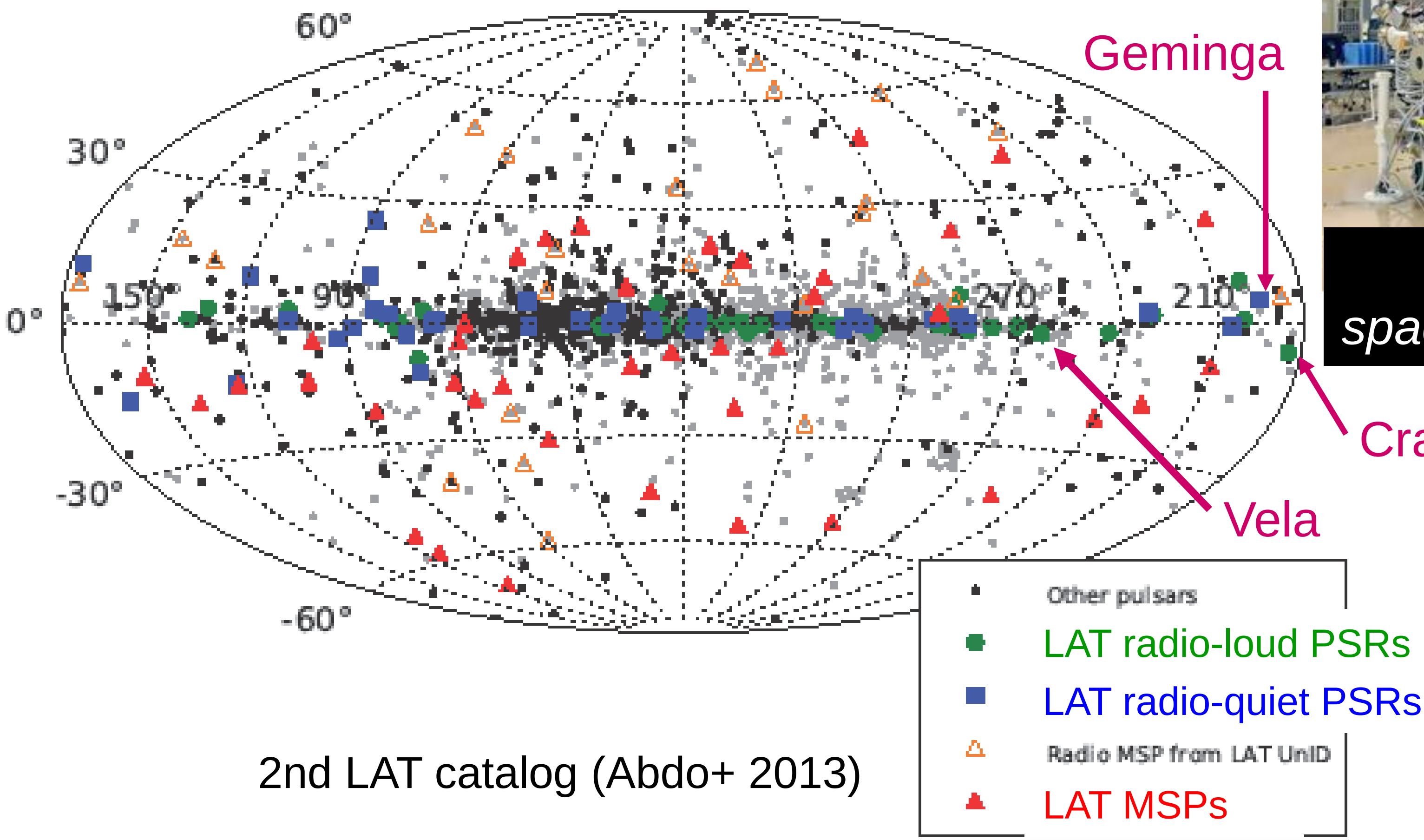

2nd LAT catalog (Abdo+ 2013)

Large Area Telescope

Fermi γ-ray space telescope

Pulsed broad-band spectra of young pulsars

- High-energy (~GeV) photons are emitted mainly via **curvature** process by ultra-relativistic, primary e^{-}'s/e^{+}'s.

(created in particle accelerator)

Fermi/LAT
(sensitive in 20 MeV – 300 GeV)

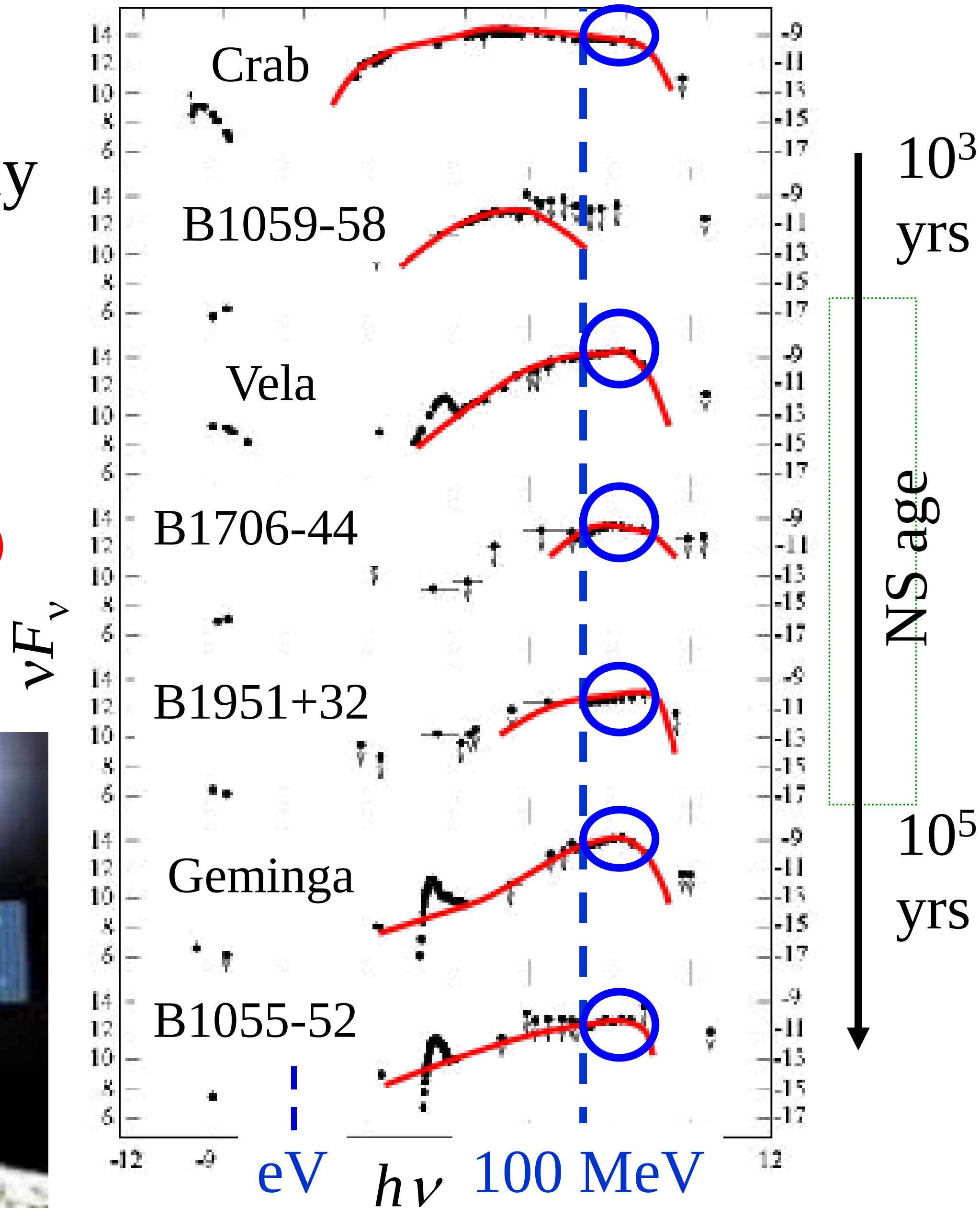

Pulsed broad-band spectra of young pulsars

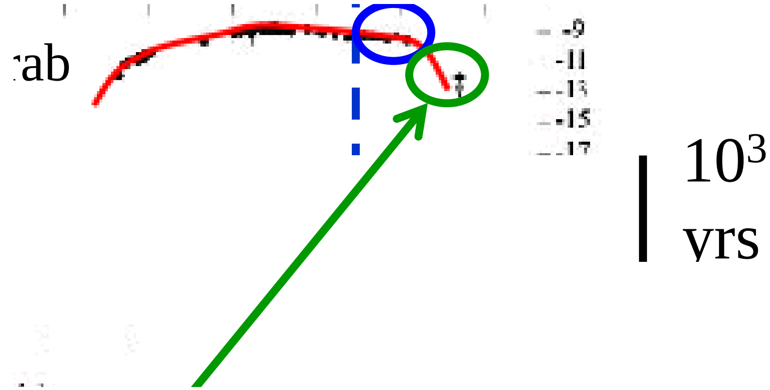

- High-energy (>100 MeV) photons are emitted mainly via **curvature** process by ultra-relativistic $e^{\pm}$'s.

- However, > 20 GeV, **Inverse-Compton scatterings (ICS) by the cascaded *e*$^{\pm}$'s** contribute.

§2 Pulsar Emission Models

Let consider how and where such incoherent, high-energy photons are emitted from pulsars.

§2 Pulsar Emission Models

If copious charges are (somehow) supplied, they realize a force-free magnetosphere, $\boldsymbol{E}\cdot\boldsymbol{B}=0$, and corotate with the magnetosphere under the corotational electric field,

$$\boldsymbol{E}_\perp \equiv -c^{-1}(\boldsymbol{\Omega}\times\boldsymbol{r})\times\boldsymbol{B}.$$

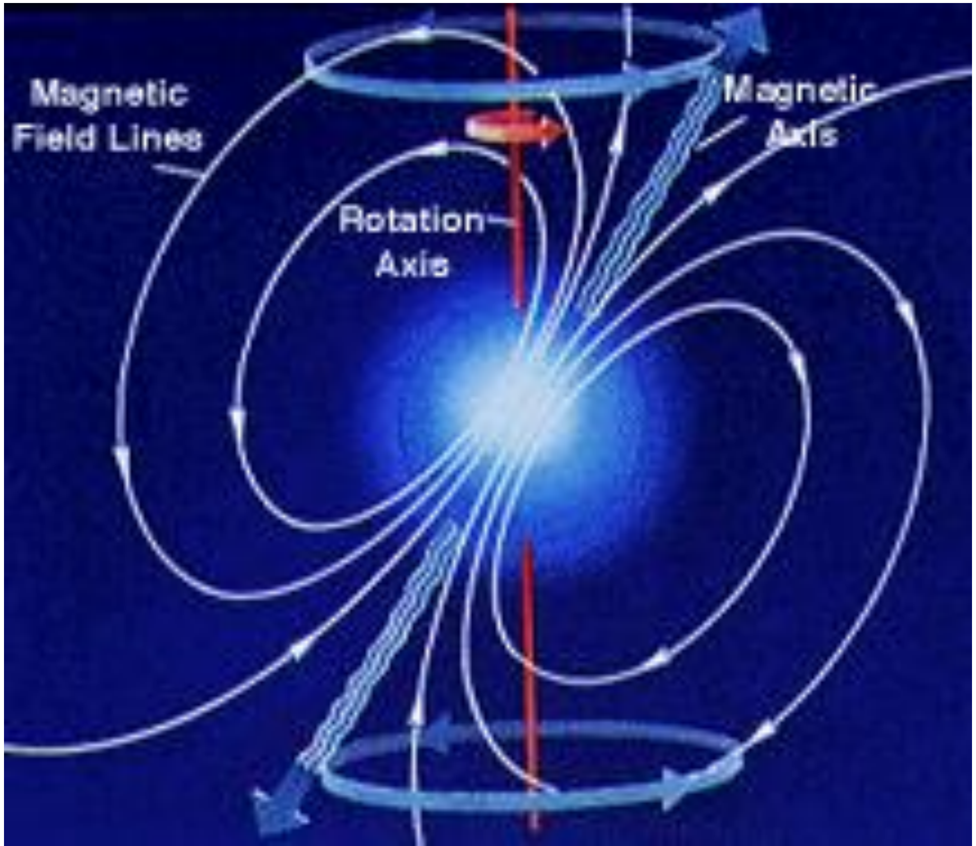

Charges corotate by $\boldsymbol{E}_\perp\times\boldsymbol{B}$ drift,

$$\boldsymbol{v}_\varphi \equiv \boldsymbol{\Omega}\times\boldsymbol{r}.$$

§2 Pulsar Emission Models

If copious charges are (somehow) supplied, they realize a force-free magnetosphere, $\boldsymbol{E}\cdot\boldsymbol{B}=0$, and corotate with the magnetosphere under the corotational electric field,

$$\boldsymbol{E}_\perp \equiv -c^{-1}(\boldsymbol{\Omega}\times\boldsymbol{r})\times\boldsymbol{B}.$$

Decoupling $\boldsymbol{E}$ into $\boldsymbol{E}_\perp$ and $\boldsymbol{E}_{\text{non-corotate}}$, we obtain from the Maxwell eq.

$$\nabla\cdot(\boldsymbol{E}_\perp+\boldsymbol{E}_{\text{non-corotate}})=4\pi\rho,$$

that is,

$$\nabla\cdot\boldsymbol{E}_{\text{non-corotate}}=4\pi(\rho-\rho_{\text{GJ}}),$$

where $\rho_{\text{GJ}}\equiv\nabla\cdot\boldsymbol{E}_\perp\sim-\boldsymbol{\Omega}\cdot\boldsymbol{B}.$

If ρ deviates from ρ_{GJ} in some region, $E_\parallel=\boldsymbol{E}_{\text{non-corotate}}\cdot\boldsymbol{B}/B$ arises around that region.

§2 Pulsar Emission Models

If copious charges are (somehow) supplied, they realize a force-free magnetosphere, $\boldsymbol{E}\cdot\boldsymbol{B}=0$, and corotate with the magnetosphere under the corotational electric field,

Thus, the problem reduces to …

"Where and how does the charge deficit ($|\rho| < |\rho_{\mathrm{GJ}}|$) appear?"

This vacuum gap ($E_{||}\neq 0$) should also account for the supply of charges that realizes the force-free magnetosphere outside of it.

If ρ deviates from ρ_{GJ} in some region,
$E_{||} = \boldsymbol{E}_{\text{non-corotate}} \cdot \boldsymbol{B}/\mathrm{B}$ arises around that region.

§2 Pulsar Emission Models

Early 80's, the polar-cap (PC) model was proposed.

(Daugherty & Harding ApJ 252, 337, 1982)

A single PC beam can produce a variety of pulse profiles.

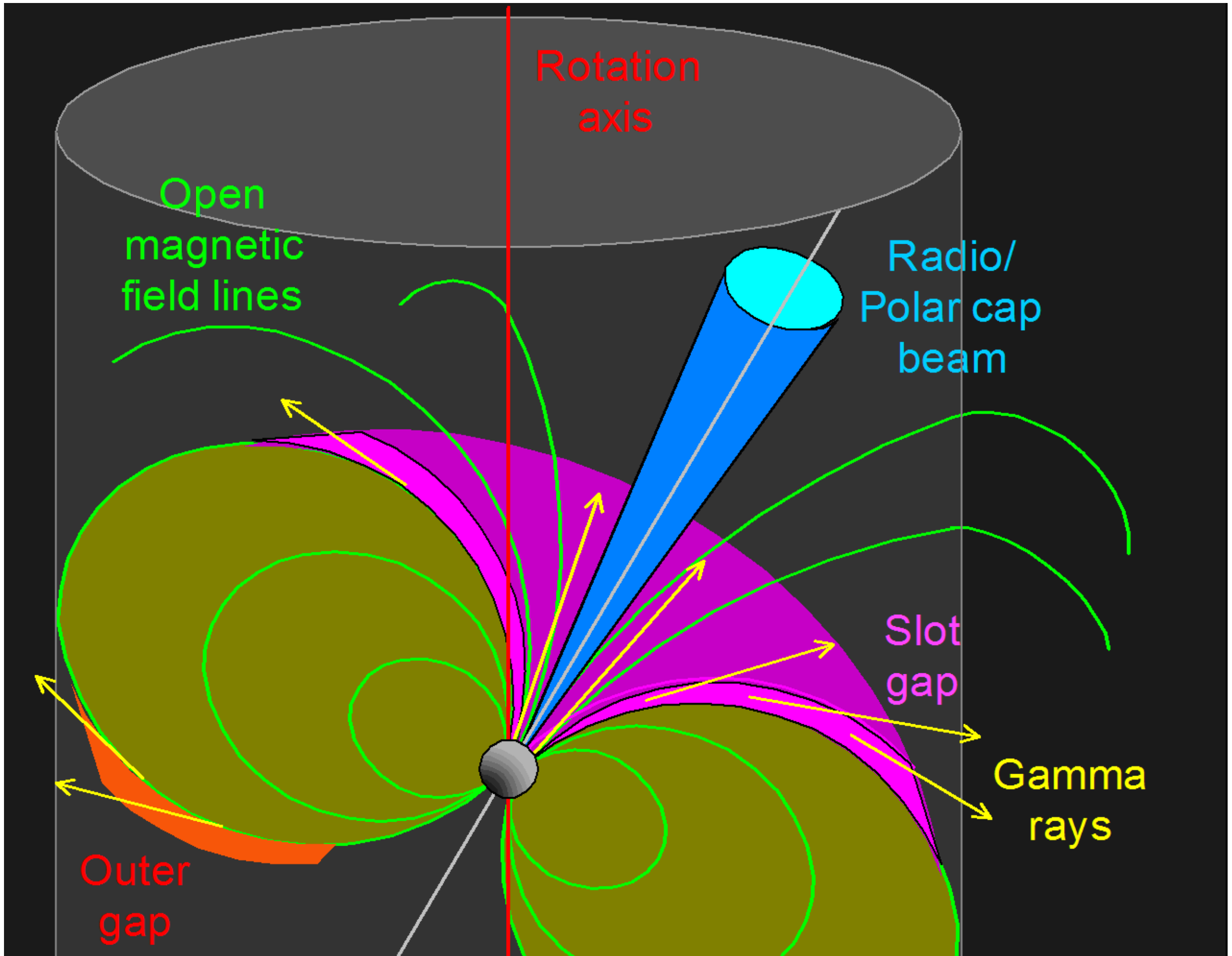

§2 Pulsar Emission Models

Early 80's, the polar-cap (PC) model was proposed.
(Daugherty & Harding ApJ 252, 337, 1982)

A single PC beam can produce a variety of pulse profiles.

However, the emission solid angle ($\Delta\Omega$ «1 ster) was too small to reproduce the wide-separated double peaks.

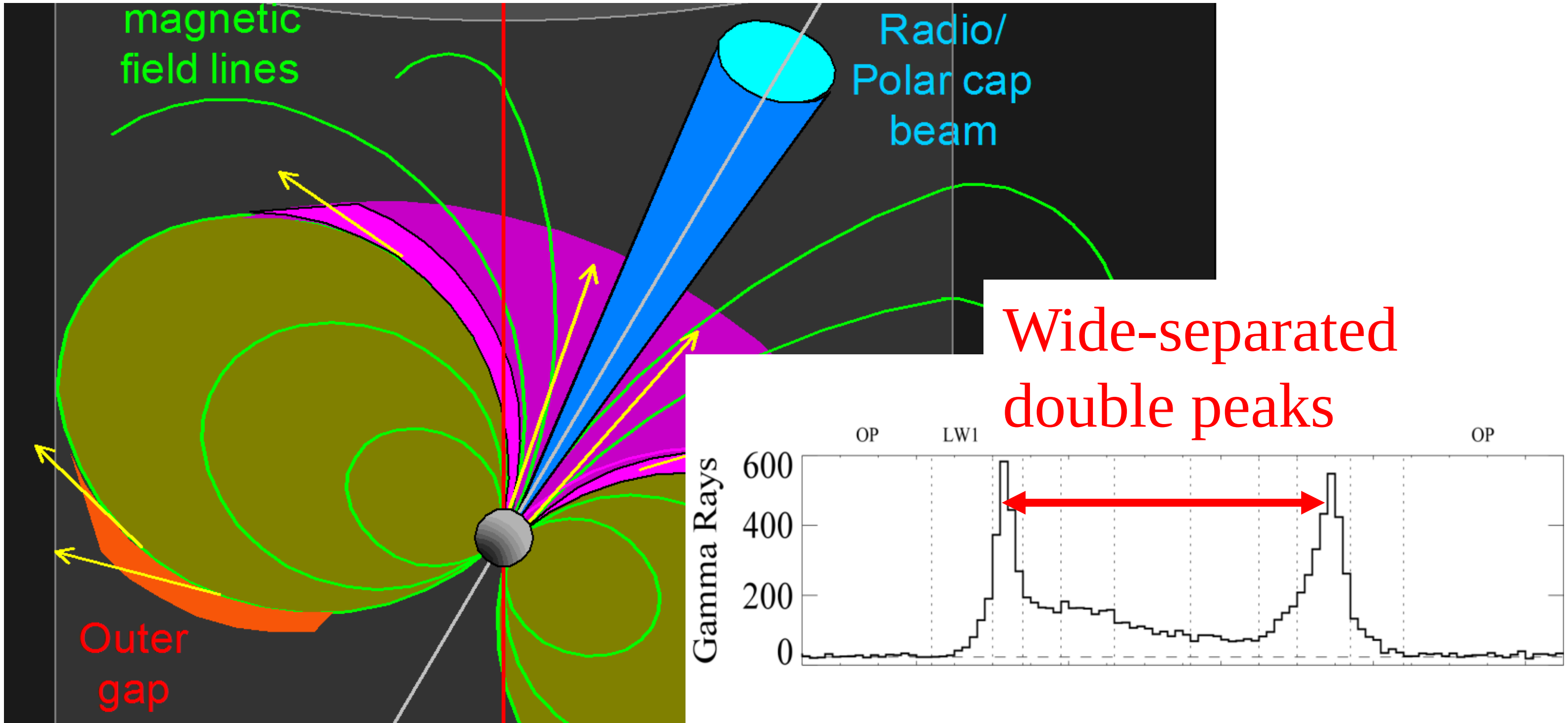

§2 Pulsar Emission Models

Early 80's, the polar-cap (PC) model was proposed.

(Daugherty & Harding ApJ 252, 337, 1982)

A single PC beam can produce a variety of pulse profiles.

However, the emission solid angle ($\Delta\Omega$ «1 ster) was too small to reproduce the wide-separated double peaks.

In addition, localization of gap altitudes («r_*) lead to too small L_γ («$0.3L_{\rm spin}$), although $L_{\rm radio}$~$10^{-5}L_{\rm spin}$ is OK.

Moreover, the detection of VHE (>20GeV) pulsed emission from the Crab pulsar, which should avoid strong magnetic absorption, clearly rules out PC emissions.

Thus, a high-altitude emission drew attention.

§2 Pulsar Emission Models

Higher-altitude emission models concentrate on …

- **slot-gap (SG) model** (Muslimov & Harding 2003, 2004)
- **pair- starved polar-cap (PSPC) model** (Venter + 2009)
- **outer gap (OG) model** (Cheng + 1986; Romani 1996)
- **striped-wind synchrotron (SWS) model** (Petri 2013)
- **wind-inverse-Compton (WIC) model** (Aharonian + 2012)

SG, PSPC models: e^- are extracted as in PC model

OG model: $e^{\pm}$'s created by γ-γ coll. and accelerated by $E_{\parallel}$

SWS model: HE pulsed photons emitted from current sheet

WIC model: VHE pulsed photons emitted via ICS by ultra-relativistic $e^{\pm}$'s accelerated at $r < 50\ R_{LC}$

§2 Pulsar Emission Models

SG model, classic OG models:

have very thin meridional thickness ($w \ll 1$),

reproduce only 10^{-1}~10^{-3} L_γ (KH 2008 ApJ 688, L25)

Therefore, the PSPC model ($w \leq 1.0$) was proposed.

However, the PSPC model contradicts with $div(\boldsymbol{B})=4\pi\rho$, in the same way as the SG model.

(KH 2011, High Energy Emission from Pulsars and Their Systems, p. 117–37)

Thus, as long as the emissions **inside LC** are concerned, the modern OG model (w>0.1), survives as the only model that quantitatively describes the pulsed HE/VHE emissions.

However, in all the models above, $\boldsymbol{B}$ configuration is <u>not</u> solved consistently with the magnetospheric currents.

§2 Pulsar Emission Models

How about the emissions **outside the light cylinder**?

In SWS or WIC model, ***B*** configuration is consistently solved with magnetospheric electric currents, whereas particle creation & radiation are artificially set up.

In the SWS model, plasma collective effects (e.g., wave-particle interactions) are considered as a heating mechanism of plasmas in the current sheet. (Chkheidze + 2013)

In the WIC model, the physical mechanism that converts the Poynting energy into the plasmas' kinetic energy has not been solved by MHD or PIC (particle-in-cell) simulations.

§2 Pulsar Emission Models

The ***B*** structure can be solved e.g., by the **PIC simulation**.

This approach is valid for **coherent pulsar radio** emissions.

(1) A bunch of electrons move in phase in PC region.

The PIC code is most suited to solve plasma collective effects from the first principles. (Timokhin & Arons 2013)

(2) Spatial size < coherent scale (<50 cm at 600 MHz)

The microscopic cell size in the PIC code favors such localized phenomena (e.g., strong shocks)

However, such exact treatment are **unnecessary** to study **incoherent high-energy** (> 0.001 eV) emissions, because

(1) plasma collective effects are negligible as $\nu > \nu_{\mathrm{plasma}}$,

(2) spatial size >1000 km for typical young pulsars.

The macroscopic PIC cell size disfavors such non-localized phenomena.

§2 Pulsar Emission Models

It is, therefore, possible to investigate incoherent pulsar HE/VHE emissions by solving the set of

(1) $e^{\pm}$ Boltzmann equations,

(2) radiative transfer equation, and

(3) the Poisson equation for the electro-static potential (i.e., one of the Maxwell equations),

without taking account of plasma collective effects in the Boltzmann equations.

Instead of solving the ***B*** field configuration near the light cylinder, we parameterize how the vacuum dipole ***B*** field is deformed into monopole-like, and compare the prediction with the γ-ray observations.

§2 *Pulsar Emission Models*

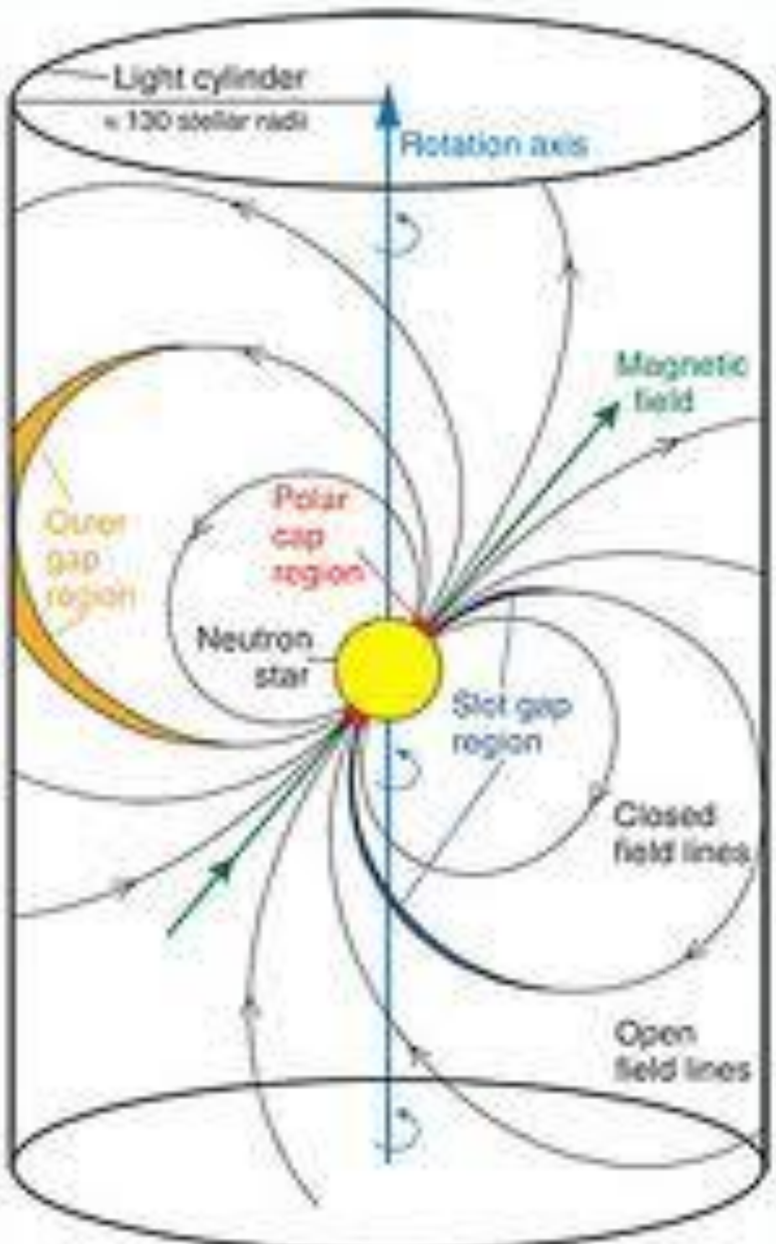

As a model of high-altitude emissions, we investigate the outer gap scenario.

Cheng, Ho, Ruderman (1986, ApJ 300, 500)

Emission altitude
~ light cylinder
⟶ hollow cone emission
($\Delta\Omega > 1$ ster)

OG model was further developed by including special relativistic effects.

Romani (1996, ApJ 470, 469)

§2 Pulsar Emission Models

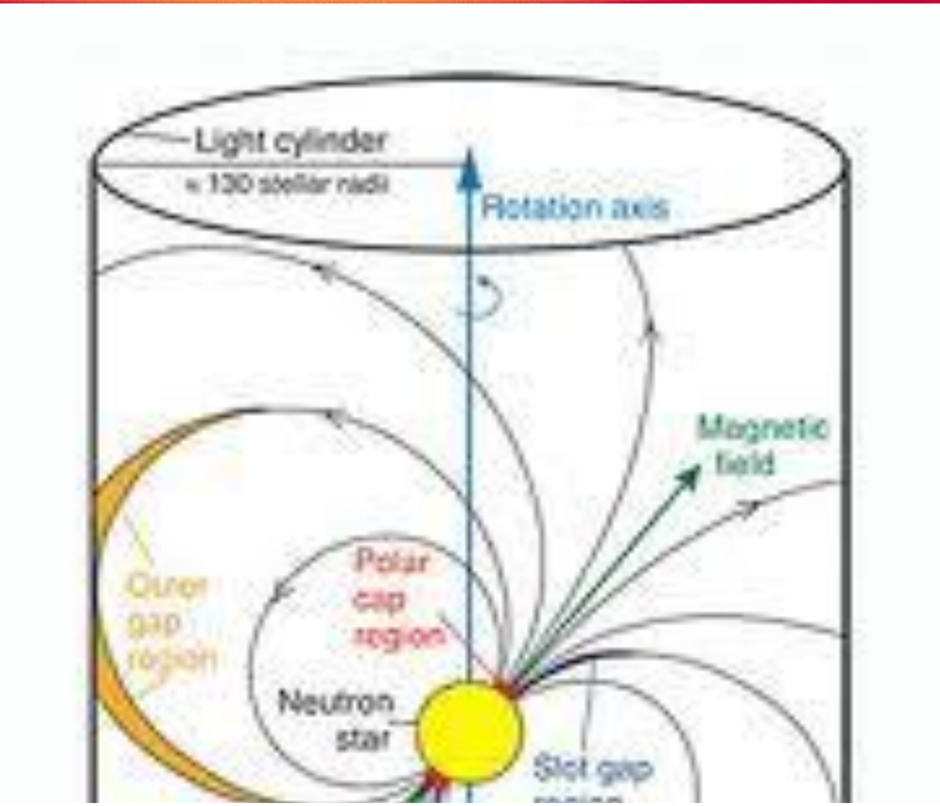

As a model of high-altitude emissions, we investigate the outer gap scenario.

Cheng, Ho, Ruderman (1986, ApJ 300, 500)

Emission altitude
~ light cylinder
⟶ hollow cone emission
($\Delta\Omega > 1$ ster)

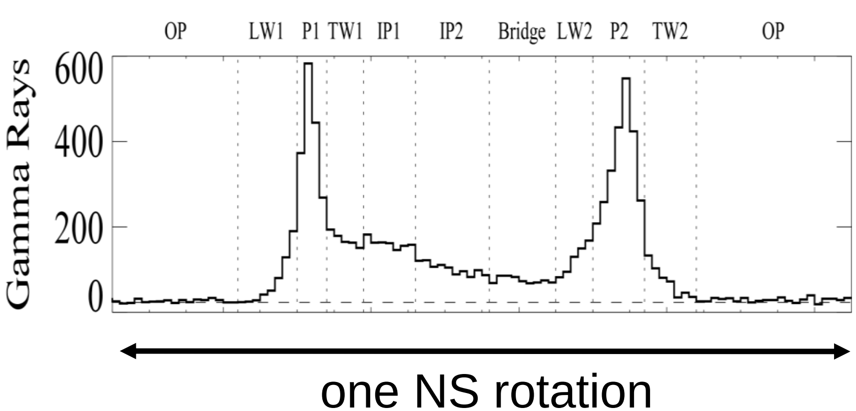

Successfully explained wide-separated double peaks.

OG model became promising.

§3 Modern Outer-gap Model: Formalism

I quantify the classic OG model by simultaneously solving the pair-production cascade in a rotating NS magnetosphere:

$e^{\pm}$'s are accelerated by $E_{||}$

Relativistic e^{+}/e^{-} emit γ-rays via synchro-curvature, and IC processes

γ-rays collide with soft photons/B to materialize as pairs in the accelerator

§3 Modern OG Model: Formalism

Poisson equation for electrostatic potential ψ :

$$-\nabla^2\psi = -\frac{\partial^2\psi}{\partial x^2} - \frac{\partial^2\psi}{\partial y^2} - \frac{\partial^2\psi}{\partial z^2} = 4\pi(\rho - \rho_{\mathrm{GJ}}) \ ,$$

where

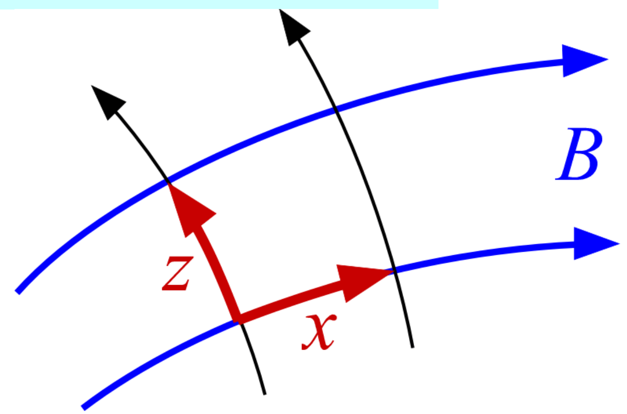

$$E_{\parallel} \equiv -\frac{\partial\psi}{\partial x} \ , \ \rho_{\mathrm{GJ}} \equiv -\frac{\mathbf{\Omega}\cdot\mathbf{B}}{2\pi c},$$

$$\rho(\mathbf{x}) \equiv e\int_1^\infty d\gamma\int_0^\pi d\chi\left[N_+(\mathbf{x},\gamma,\chi) - N_-(\mathbf{x},\gamma,\chi)\right] + \rho_{\mathrm{ion}}(\mathbf{x}),$$

$$\mathbf{x} = (x, y, z) \ .$$

N_+/N_-: distrib. func. of e^+/e^-

γ: Lorentz factor of e^+/e^-

χ: pitch angle of e^+/e^-

§3 Modern OG Model: Formalism

Assuming $\partial_t + \Omega\partial_\phi = 0$, we solve the $e^{\pm}$'s Boltzmann eqs.

$$\frac{\partial N_\pm}{\partial t} + \vec{v}\cdot\nabla N_\pm + \left(e\vec{E}_{\parallel} + \frac{\vec{v}}{c}\times\vec{B} \right)\cdot\frac{\partial N_\pm}{\partial \vec{p}} = S_{IC} + S_{SC} + \int \alpha_\nu d\nu \int \frac{I_\nu}{h\nu} d\omega$$

together with the radiative transfer equation,

$$\frac{dI_\nu}{dl} = -\alpha_\nu I_\nu + j_\nu$$

$N_\pm$: positronic/electronic spatial # density,

$E_\parallel$: mangnetic-field-aligned electric field,

S_{IC}: ICS re-distribution function, $d\omega$: solid angle element,

I_ν: specific intensity, l : path length along the ray

α_ν: absorption coefficient, j_ν: emission coefficient

§3 Application to the Crab pulsar

This numerical scheme can be applied to arbitrary pulsars. Today, we apply it to the Crab pulsar.

Recent force-free, MHD, and PIC simulations suggest that ***B*** field approaches **monopole-like** near and beyond the light cylinder.

Thus, we consider

vacuum, rotating dipole ***B***

+ *b* * split-monopole ***B*** (Michael'74)

b=0: pure dipole

b=1: $B_{\mathrm{dipole}}=B_{\mathrm{monopole}}$ @ LC

§3 Application to the Crab pulsar

First, let us see why the double-peak light curve is formed.
Examine the vacuum (i.e., non-screened) solution of $E_{\parallel}$.

$E_{\parallel}$ for vacuum, rotating dipole ***B*** field (*b*=0 case)

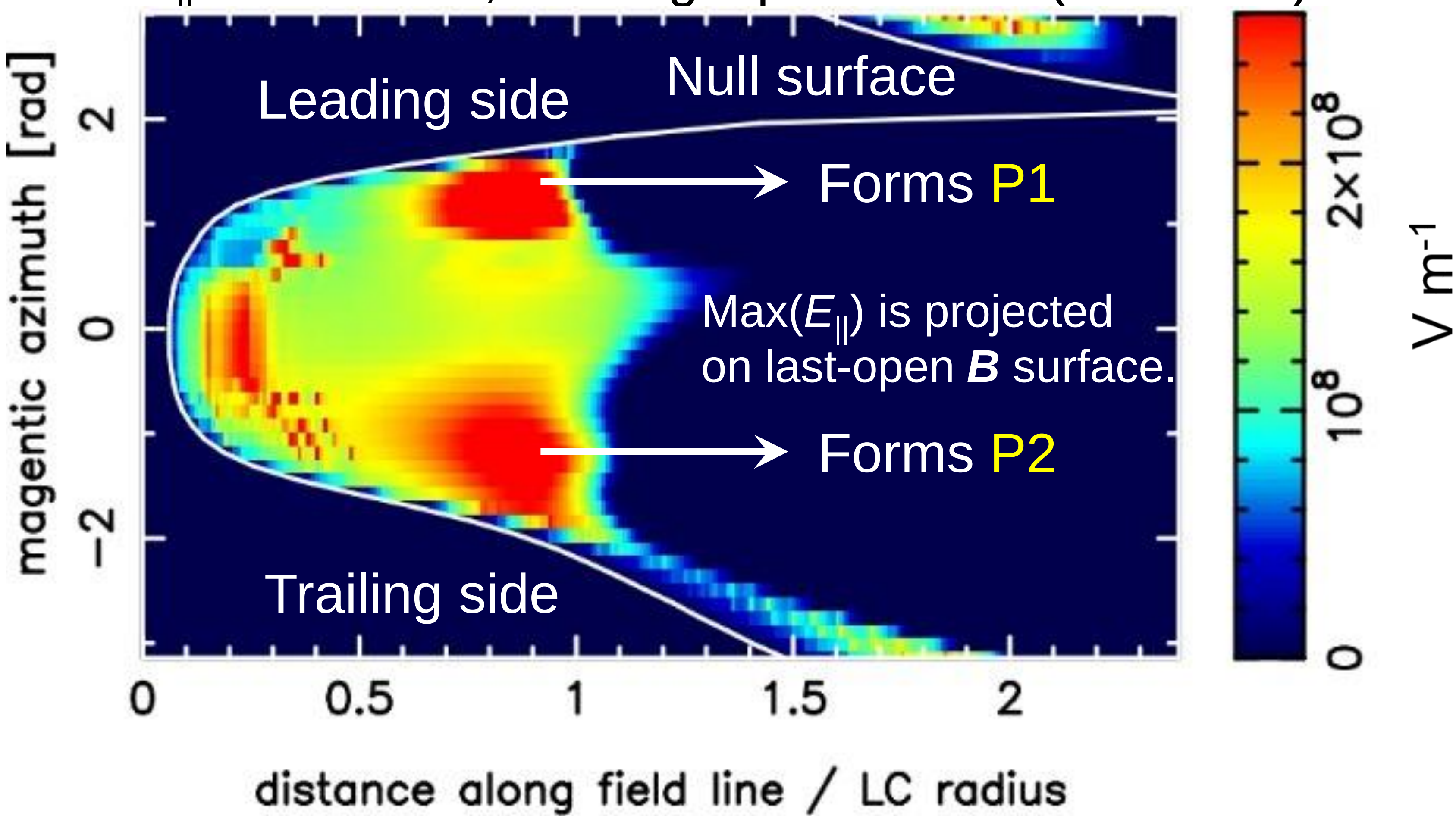

§3 Application to the Crab pulsar

$E_\parallel$ is governed by the ρ_{GJ} distribution, which is solely determined by $\boldsymbol{B}$ geometry.

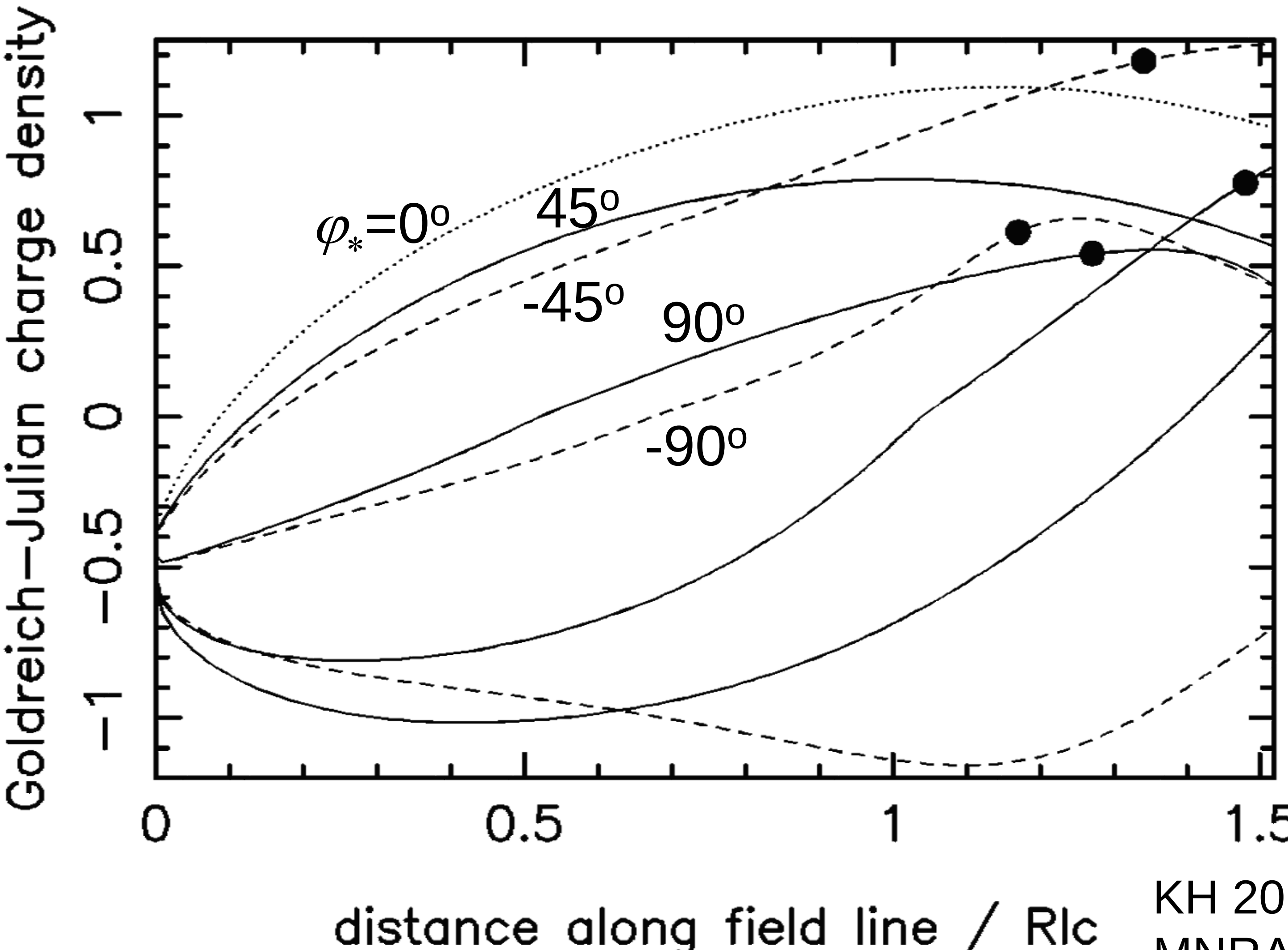

Pure dipole b=0.

KH 2014, MNRAS 442, L43

§3 Application to the Crab pulsar

$E_{\parallel}$ is governed by the ρ_{GJ} distribution, which is solely determined by ***B*** geometry.

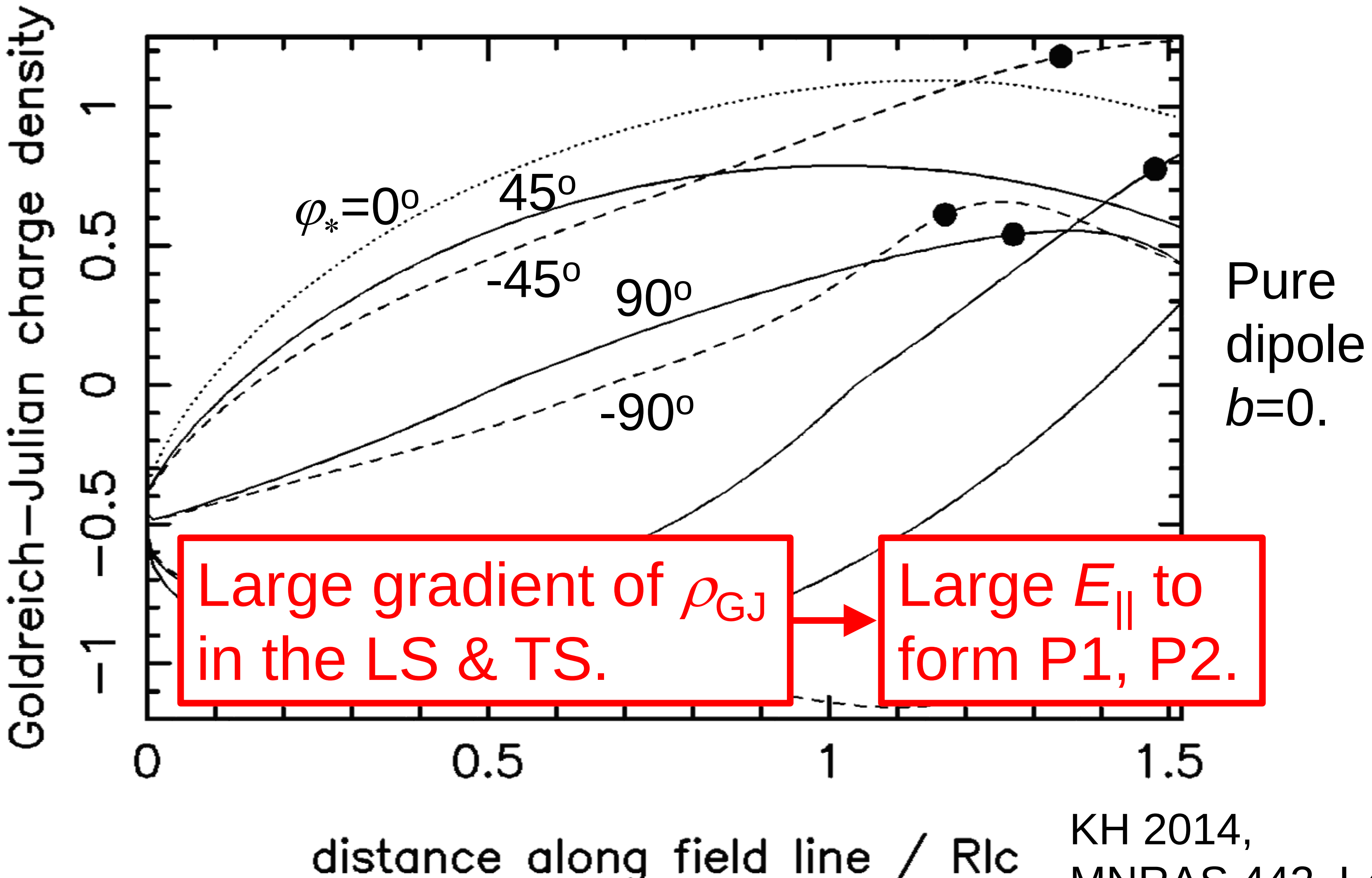

KH 2014, MNRAS 442, L43

§5 Application to the Crab pulsar

$E_{||}$ is heavily screened by the produced pairs. Nevertheless, the essential features of P1/P2 formation is unchanged.

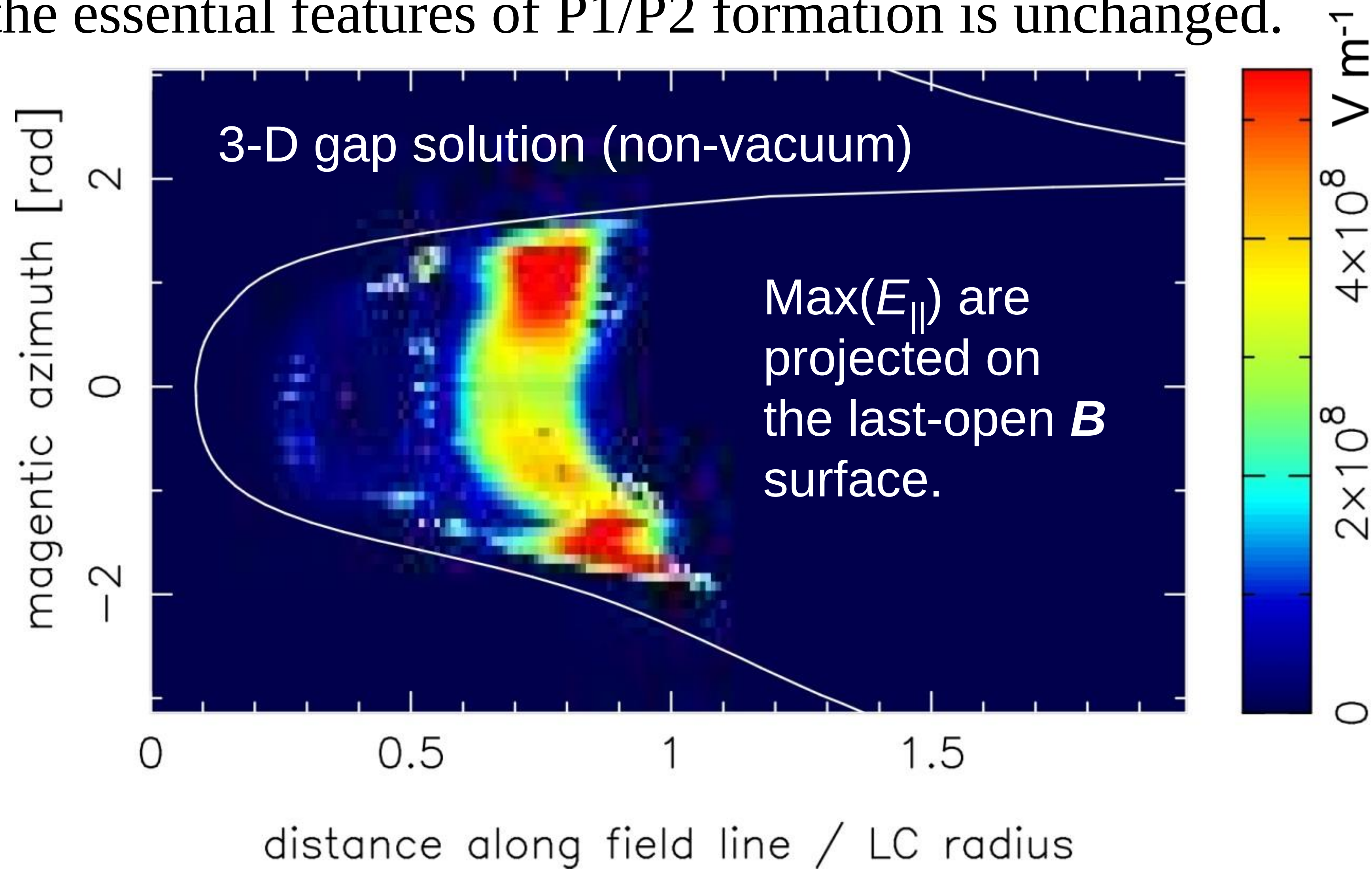

§4 Results: pulse profiles

The resultant γ-ray light curves changes as a function of the observer's viewing angles:

b=0 (pure rotating vacuum dipole)

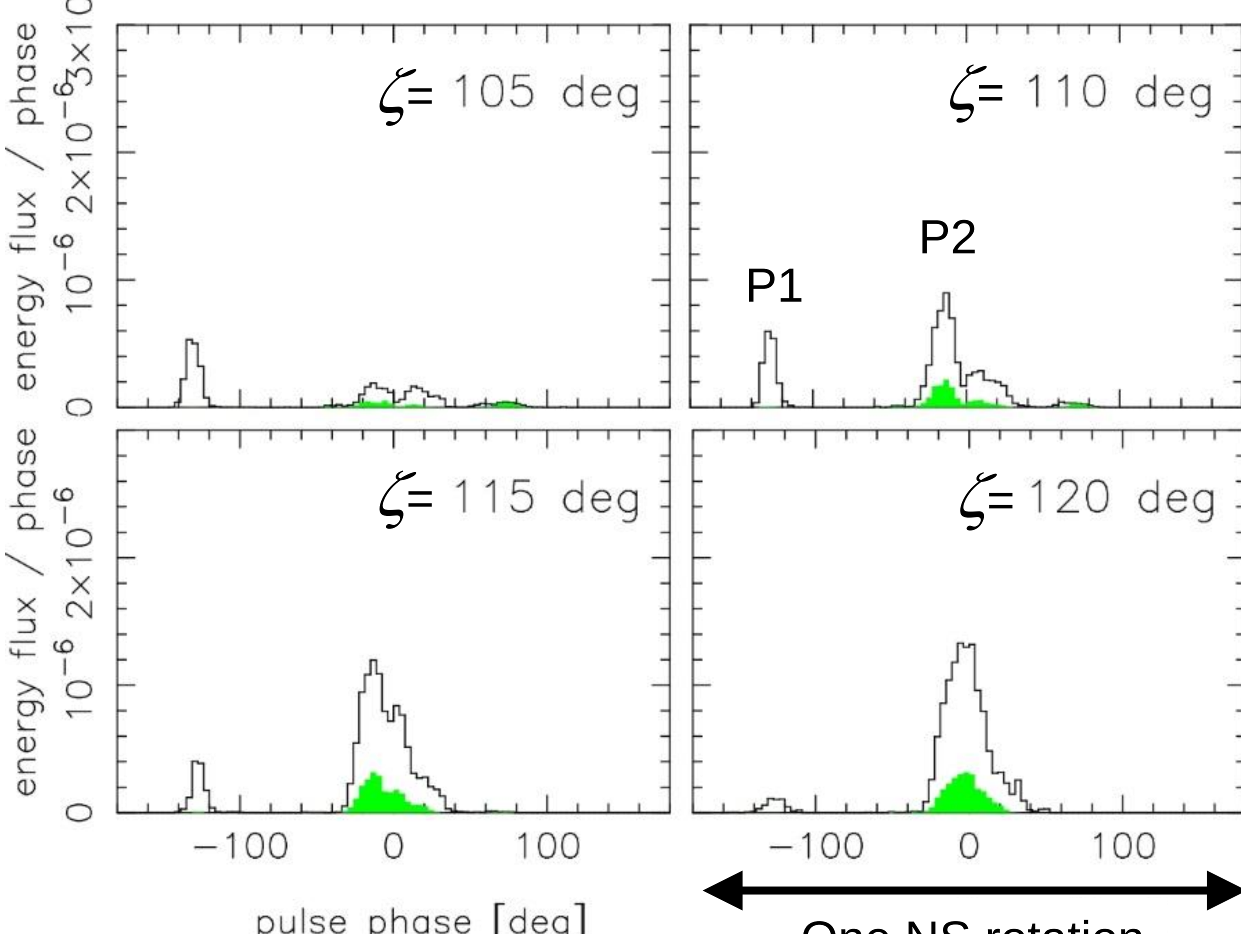

One NS rotation

B inclination:
α=65°

0.1-30 GeV
>30 GeV (x10)

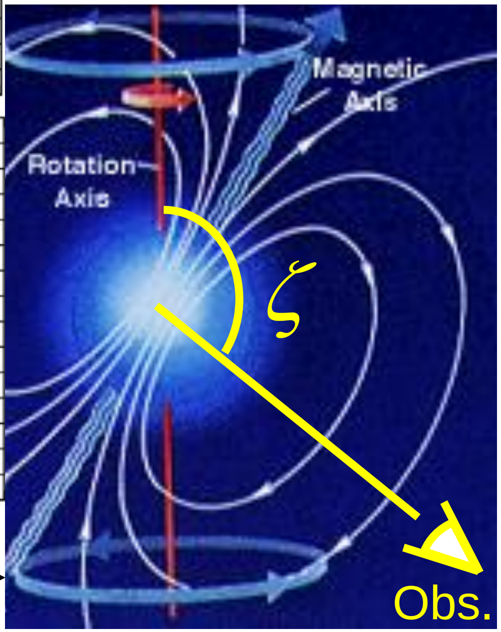

§4 Results: pulse profiles

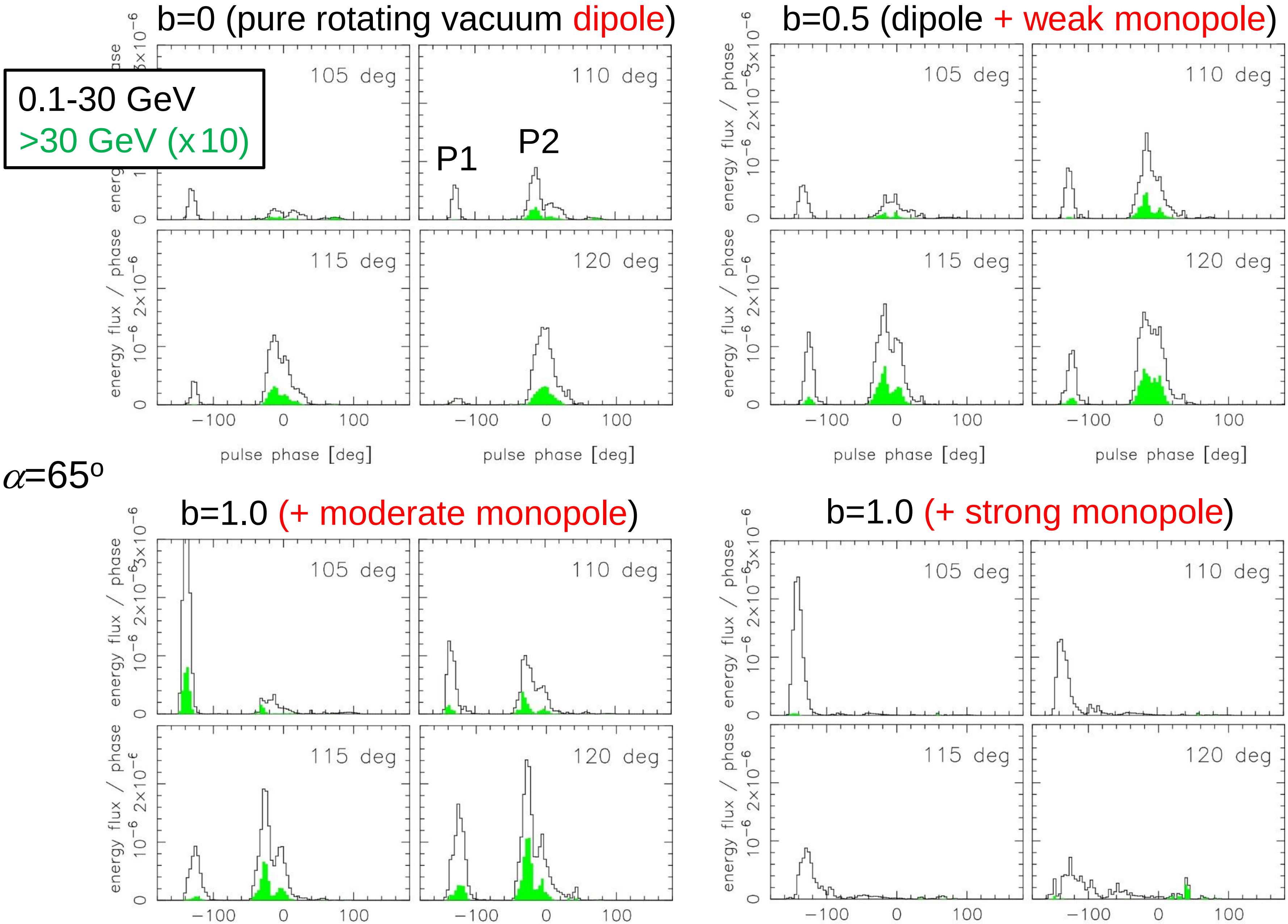

§4 Results: pulse profiles

b=0 (pure rotating vacuum dipole)

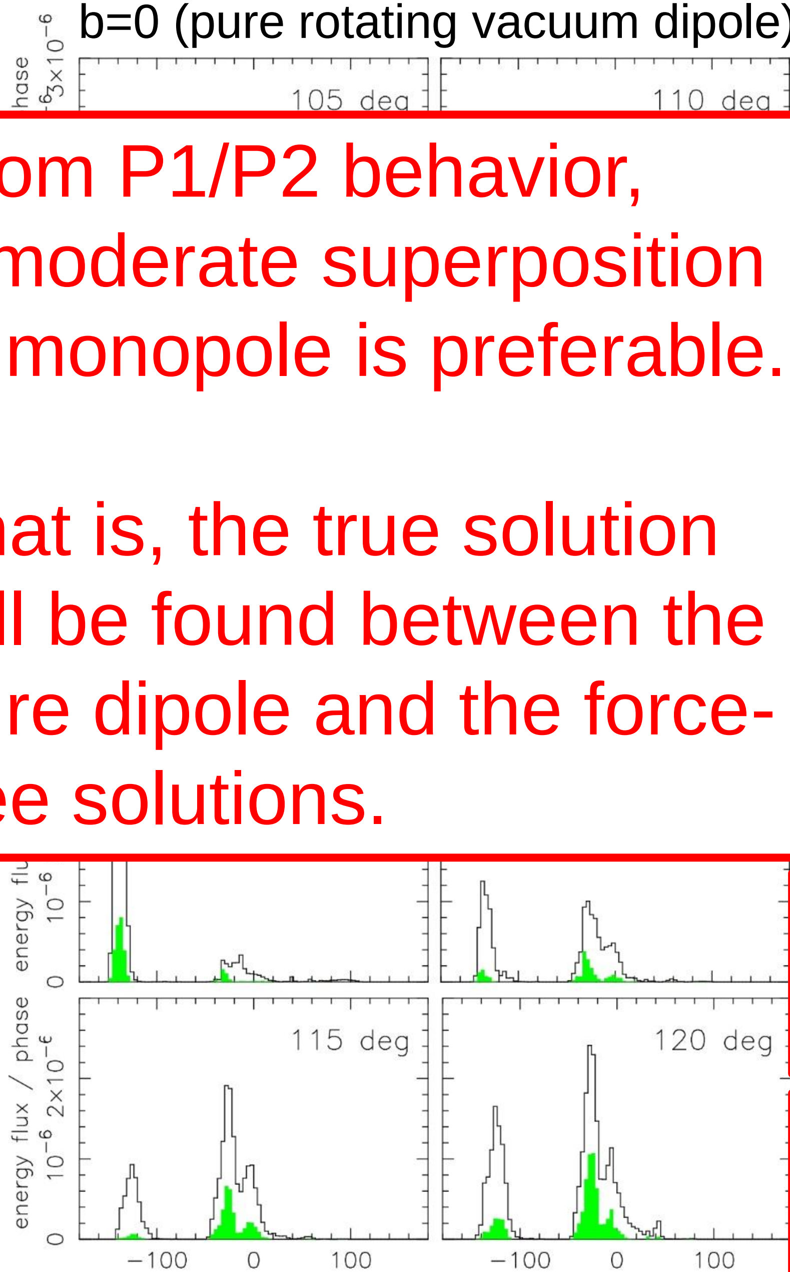

From P1/P2 behavior,
a moderate superposition
of monopole is preferable.

That is, the true solution
will be found between the
pure dipole and the force-
free solutions.

b=0.5 (dipole + weak monopole)

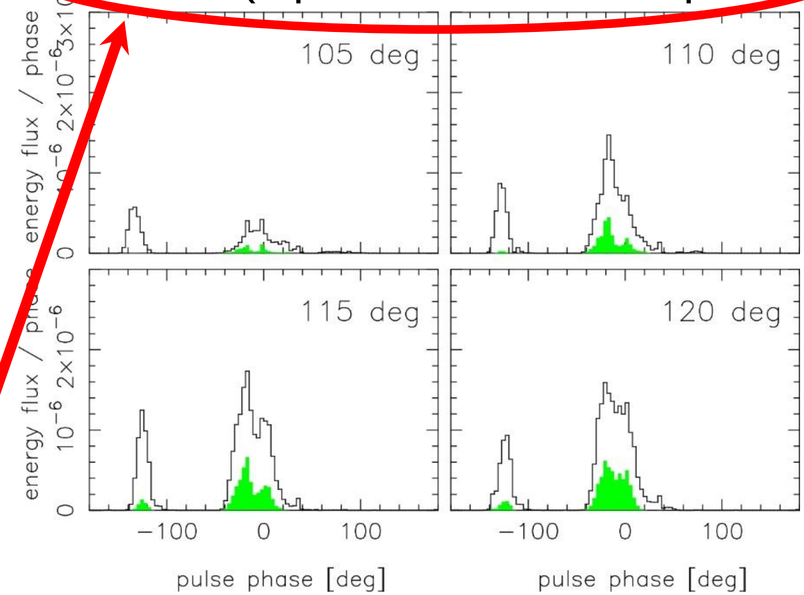

b=1.0 (+ strong monopole)

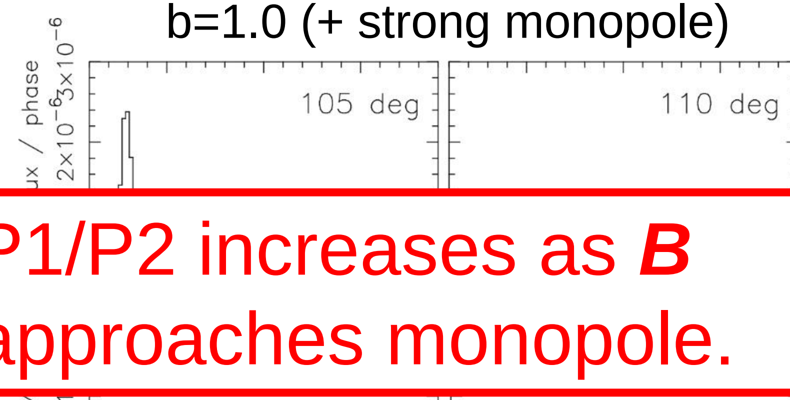

P1/P2 increases as ***B*** approaches monopole.

P1/P2 decreases with increasing photon energy.

§4 Results: pulse profiles

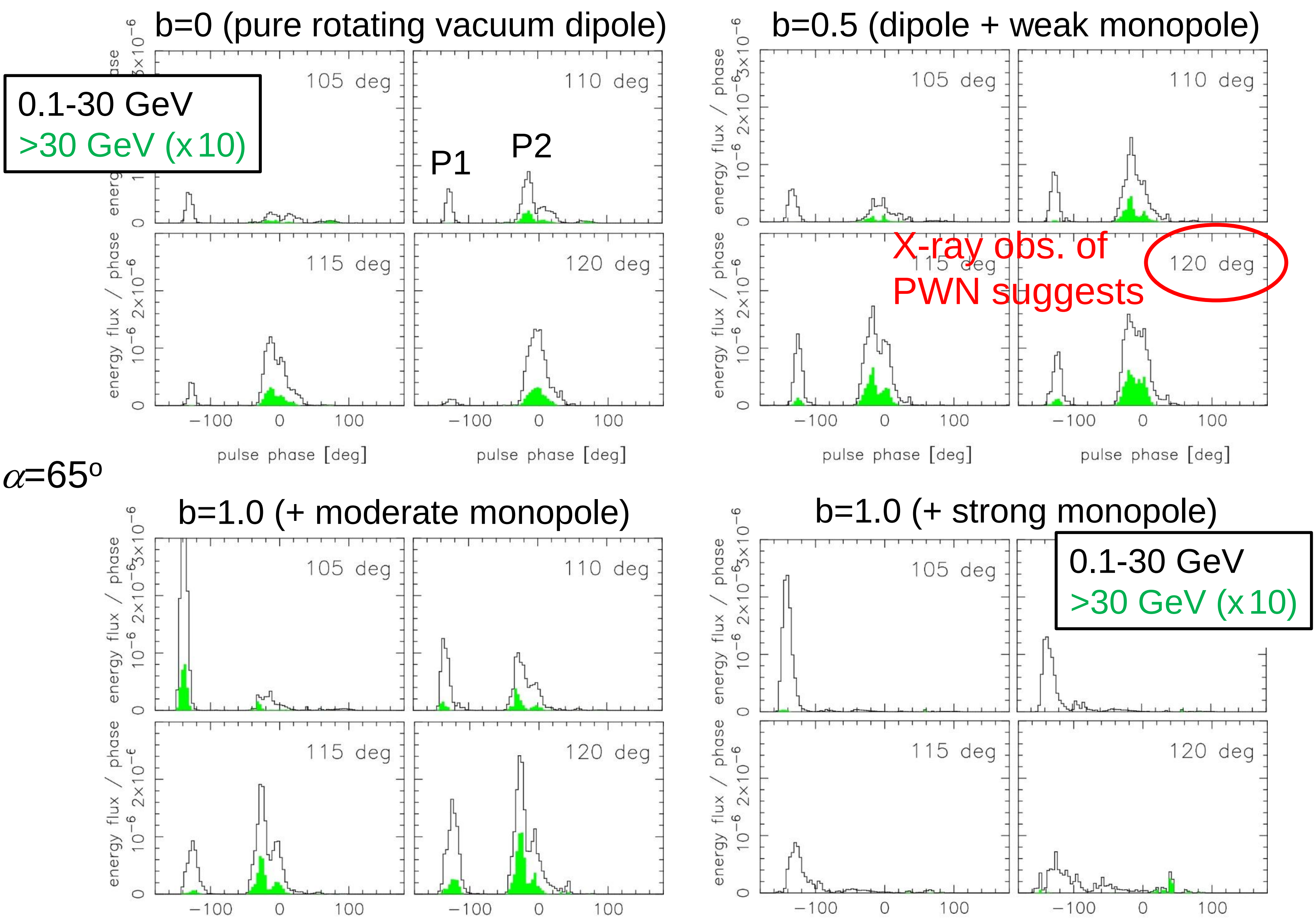

§4 Results: pulse profiles

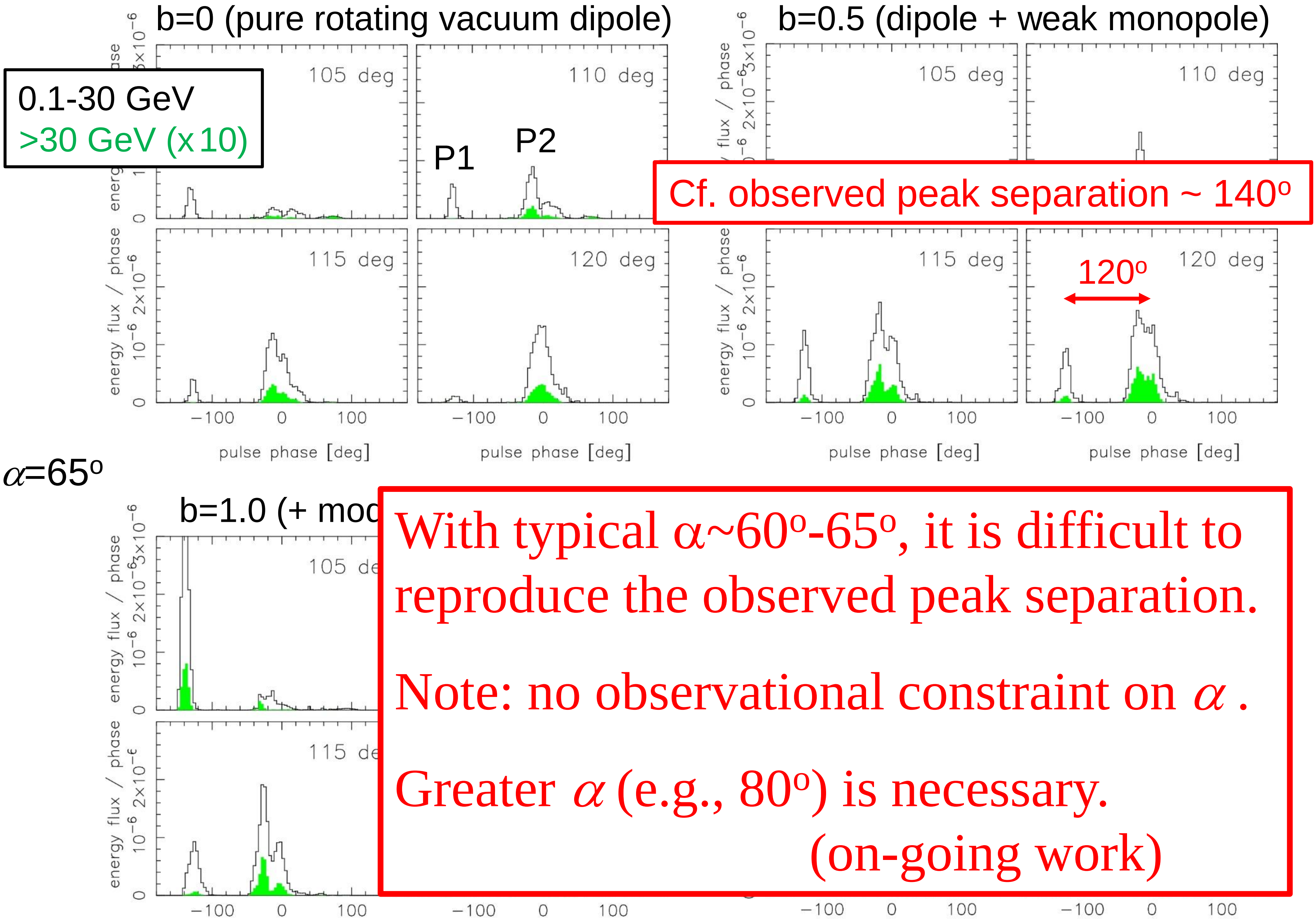

With typical α~60°-65°, it is difficult to reproduce the observed peak separation.

Note: no observational constraint on α .

Greater α (e.g., 80°) is necessary.

(on-going work)

§8 Results: Application to the Crab pulsar

Total and phase-resolved spectrum for $b=0$, $\alpha=60^{\circ}$, $\zeta=95^{\circ}$

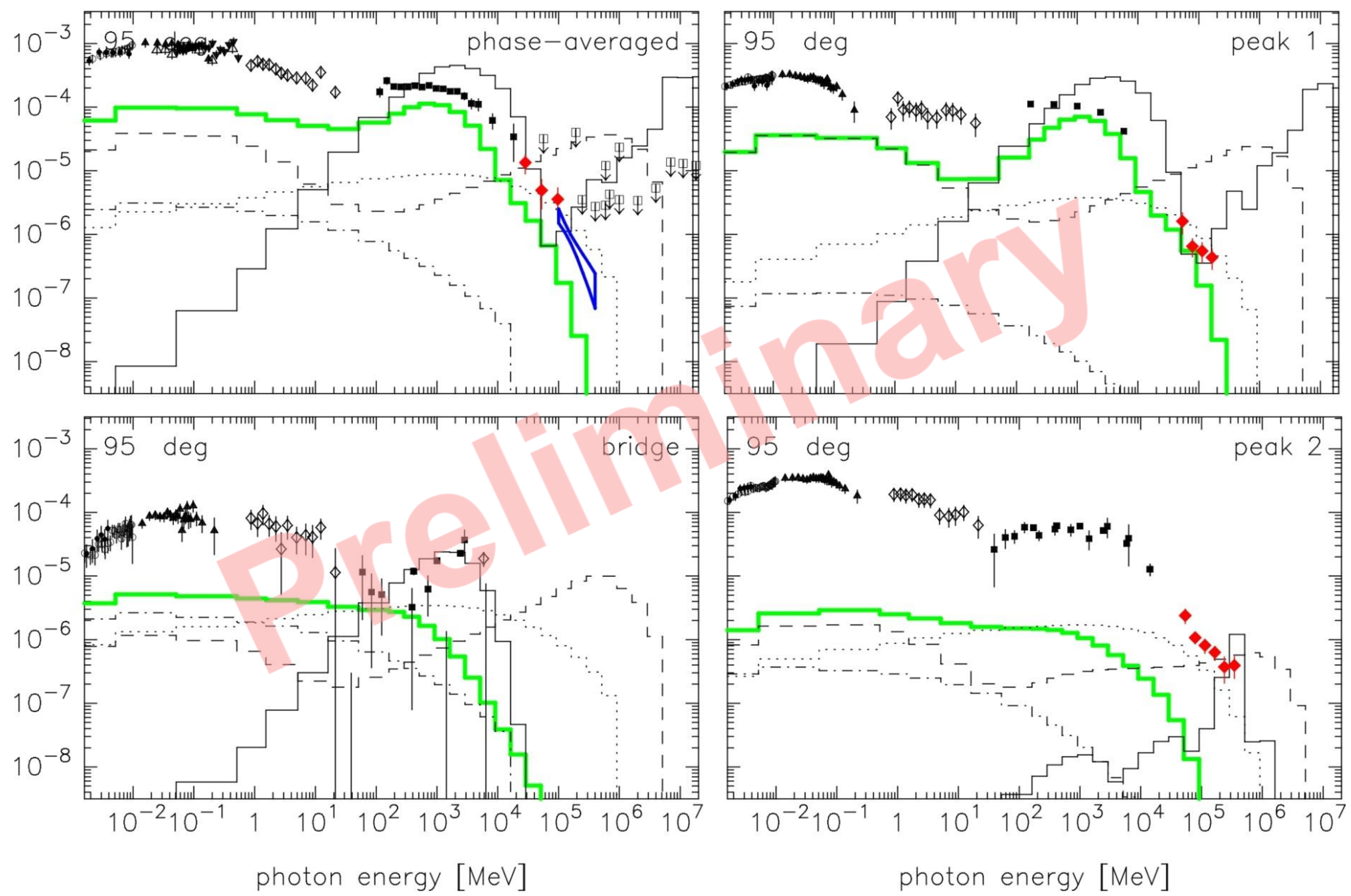

§8 Results: Application to the Crab pulsar

Total and phase-resolved spectrum for b=0, α=60°, ζ=100°

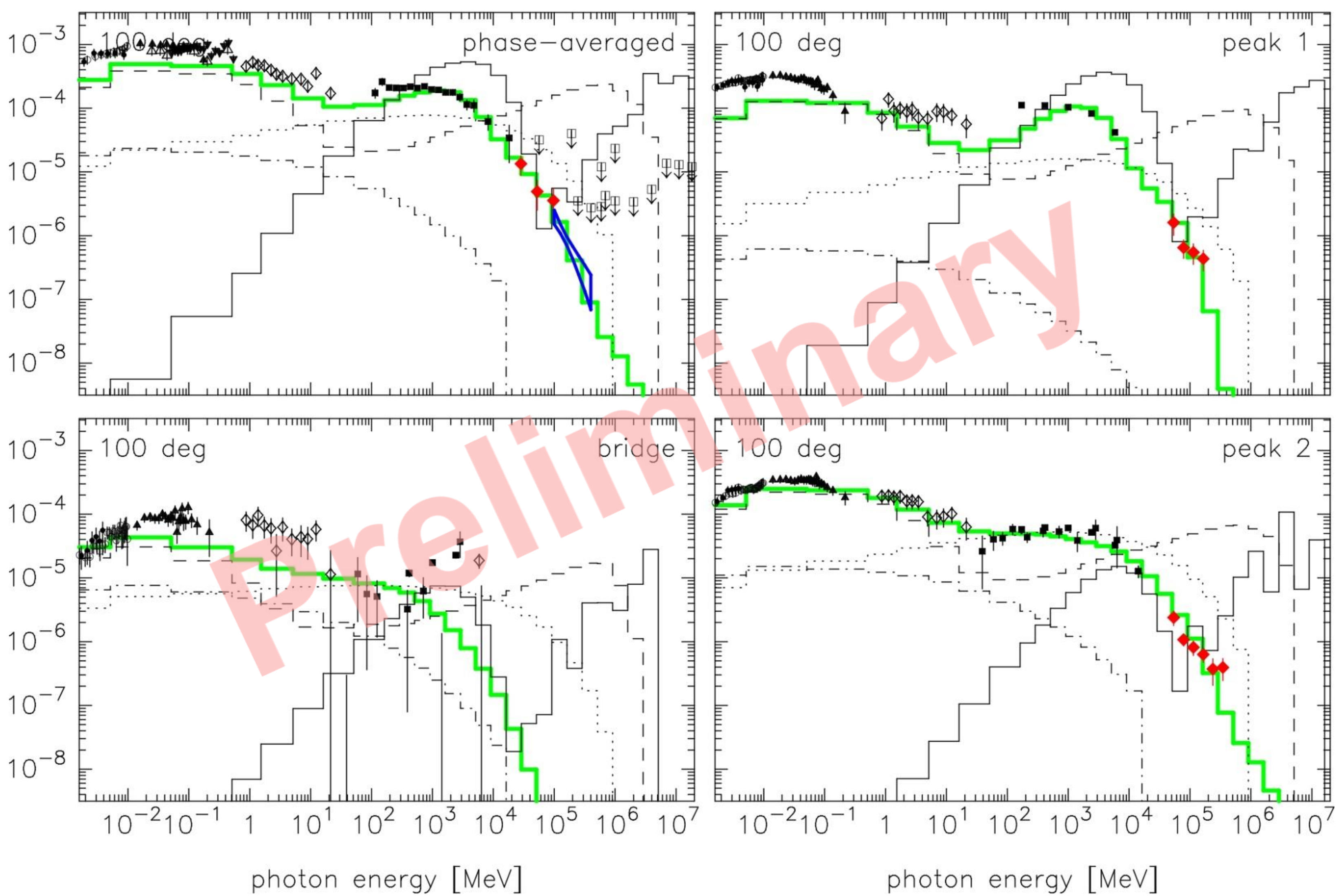

§8 Results: Application to the Crab pulsar

Total and phase-resolved spectrum for $b=0$, $\alpha=60^{\circ}$, $\zeta=105^{\circ}$

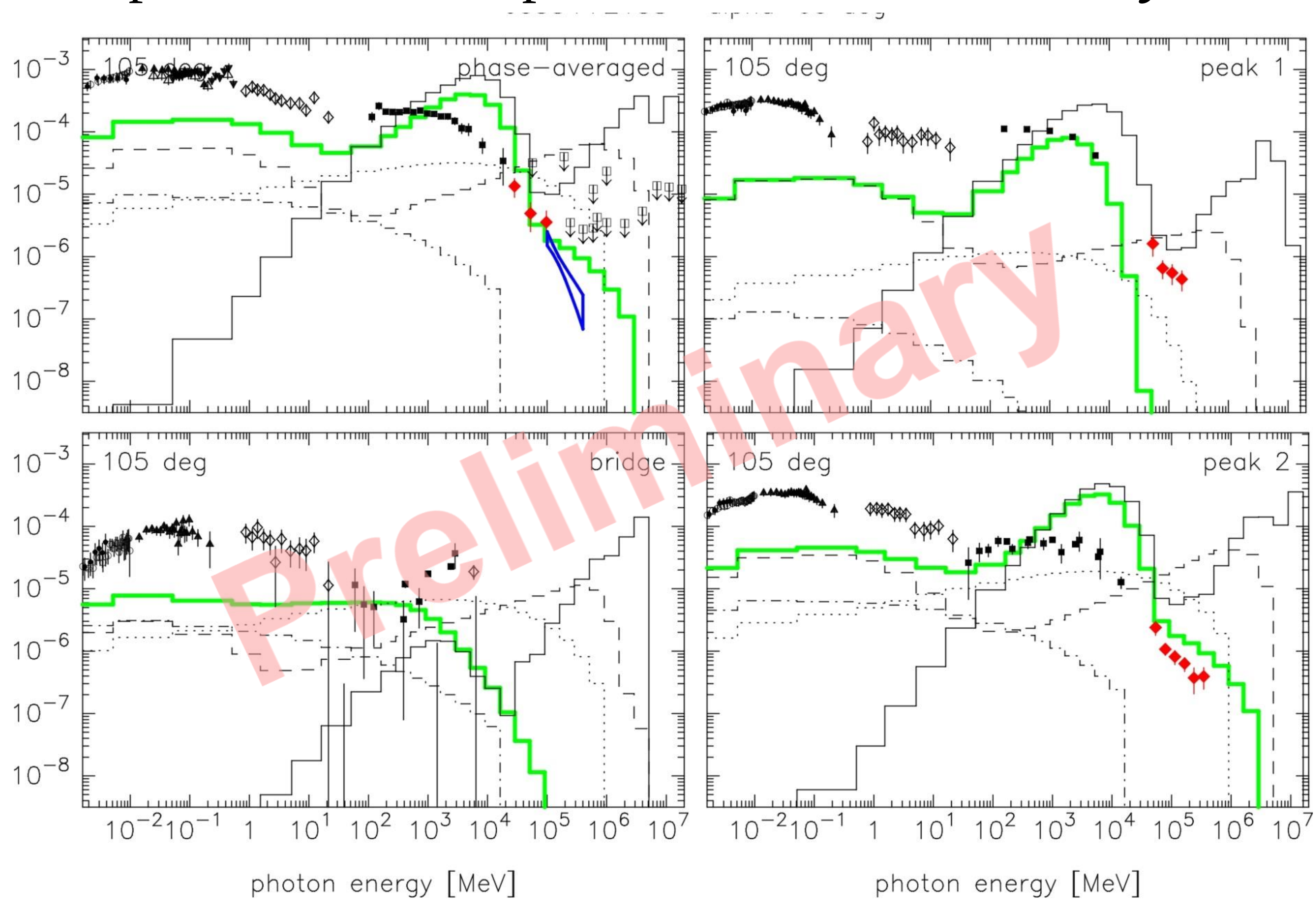

Summary

- We can predict the HE/VHE emissions from pulsar outer magnetospheres, by solving the set of Maxwell (div$\boldsymbol{E}=4\pi\rho$) and $e^{\pm}$ Boltzmann eqs., radiative transfer eq., if we specify P, dP/dt, α_{incl}, kT_{NS}.
- The solution corresponds to a quantitative extension of classic outer gap model. We no longer have to assume the gap geometry, $E_{||}$, $e^{\pm}$ distribution functions.
- Moderate $\boldsymbol{B}$ deformation (b~0.5) near LC is preferable to reproduce P1/P2 ratio and relatively large peak separation.
- Bridge emission reduces due to strong screening.
- For $\zeta=120^{\mathrm{o}}$ (as inferred from X-ray torus obs.), Crab pulsar's γ-ray peak separation becomes < 120^{o} for $\alpha<65^{\mathrm{o}}$, whereas it should be ~140^{o}. ($\alpha=70^{\mathrm{o}}$-80^{o} cases are on-going.)
- If $\zeta=100^{\mathrm{o}}$, $\alpha=60^{\mathrm{o}}$ with $b=0$ (dipole) gives an acceptable fit.